

Effects of Potential Driving Factors on Surface Solar Radiation Trends over China in Recent Years

QIUYAN WANG,^{a, b, c} HUA ZHANG,^{b, *} MARTIN WILD,^c QI CHEN,^b XIXUN ZHOU,^b GUANGYU SHI,^{a, d} AND YUEMING CHENG^e

^a Collaborative Innovation Center on Forecast and Evaluation of Meteorological Disasters, Nanjing University of Information Science and Technology, Nanjing, China

^b State Key Laboratory of Severe Weather, Chinese Academy of Meteorological Sciences, Beijing, China

^c Institute for Atmospheric and Climate Science, ETH Zurich, Zurich, Switzerland

^d State Key Laboratory of Numerical Modeling for Atmospheric Sciences and Geophysical Fluid Dynamics, Institute of Atmospheric Physics, Chinese Academy of Sciences, Beijing, China

^e Key Laboratory of Meteorological Disaster of Ministry of Education, Nanjing University of Information Science and Technology, Nanjing, China

Abstract

The annual mean surface solar radiation (SSR) trends under all-sky, clear-sky, all-sky-no-aerosol, and clear-sky-no-aerosol conditions as well as their possible causes are analyzed over China for 2005-2018 based on different satellite-retrieved datasets to determine the likely driver of the trends. Then, the relative contributions from different cloud types to the cloud-cover-induced SSR trends are further explored in four typical sub-regions at both annual and seasonal time scales by using a radiative transfer model.

Our satellite-derived results show that the increasing SSR trends under all-sky condition over most regions of northern China are mainly caused by the combined effects of clouds and aerosols, although aerosols play a more important role in some individual regions. However, cloud (aerosol) effects contribute more to the all-sky SSR declines (increases) over southern China. Besides, clouds and aerosols are the primary factors of the all-sky SSR trends over China compared with water vapor and ozone. Our simulations point out that the decreases in low cloud cover (LCC) over the North China Plain are the largest positive contributor of all cloud types to the marked annual and seasonal cloud-cover-induced SSR increases, and the positive contributions from both high cloud cover (HCC) and LCC declines in summer and winter greatly contribute to the simulated cloud-cover-induced SSR increases over East China. The contributions from medium-low cloud cover (mid-LCC) and LCC variations dominate the cloud-cover-caused SSR trends over the southwestern and South China throughout the seasons, except for the larger HCC contribution in summer.

Data and Method

TABLE 1. Summary of inputs used in the BCC_RAD model.

| Variables | Data sources | Spatial and Temporal resolution | Dimensions | Level ranges |
|---|-----------------------|----------------------------------|---------------|----------------------------------|
| H ₂ O O ₃ 、T CO ₂ 、CH ₄ | AIRS L3 | 1°×1°/ monthly | lev, lat, lon | 1000 - 100 hPa 1000 - 0.1 hPa |
| H ₂ O O ₃ 、T | MERRA2 | 1°×1°/ monthly | | 100 - 0.1 hPa 1 - 0.1 hPa |
| Surface albedo Surface pressure 2-meter temperature Skin temperature | ERA-Interim | 1°×1°/ monthly | lat, lon | None |
| Solar Zenith angle Liquid water/Ice Cloud effective radius Aerosol optical depth at 550 nm | MODIS/Aqua | 1°×1°/monthly | lat, lon | None |
| Liquid water/ice content Total/High/Mid-Low cloud fraction | CloudSat CERES SYN | 2.8°×2.8°/daily 1°×1°/monthly | lat, lon | None |

To calculate the effects of long-term changes in different potential driving factors (e.g., cloud cover, AOD, water vapor, and ozone) on SSR trends quantitatively during 2005-2018 in China, the observed annual or seasonal means of these factors for each year from 2005 to 2018, along with their counterparts of multi-year averages of profiles, solar zenith angle, and surface albedo, were used as inputs into the BCC_RAD radiative transfer model, respectively.

The concept of relative trend percentage was utilized to avoid the differences in absolute values between different model assumptions.

$$Relative\ Trend\ Percentage_K = \frac{Trend_K}{\sum abs(Trend_i)} \times 100\% \quad (1)$$

Where the subscript i (k) denotes all (one) of the SSR trends mentioned below, and the denominator represents the summation of absolute values of either the simulated SSR trends caused by the changes in TCC, AOD, water vapor, and ozone, or the SSR trends under all-sky-no-aerosol, clear-sky, and clear-sky-no-aerosol conditions from CERES-derived product, or the SSR trends induced by the HCC, mid-HCC, mid-LCC, and LCC changes for simulating contributions from different cloud types, respectively.

Conclusions

Our results suggest that clouds and aerosols play primary roles in the satellite-derived SSR trends during 2005-2018 over China, while the impacts of water vapor and ozone on the SSR trends are much smaller in their magnitudes.

The simulated relative SSR trends caused by clouds and aerosols are generally in line with the corresponding relative trends derived from CERES products, despite some existing discrepancies in their distributions and magnitudes over some regions. The model assumptions, different input data sources, and inadequacies in the assumptions with respect to the vertical cloud overlaps as well as the interactions between clouds and aerosols in the radiative transfer model are likely causes for these differences.

The relative contributions from different cloud types to cloud-cover-induced SSR trends over China in recent years mainly depend on regions and seasons, and the changes in HCC contribute more to the SSR trends in summer over most regions, which is possibly associated with the deep convection in the season. However, the contributions from LCC or mid-LCC are responsible for the cloud-cover-caused SSR trends over most regions in China throughout the seasons.

Results - Analyses of satellite-derived SSR trends under different conditions and their potential causes

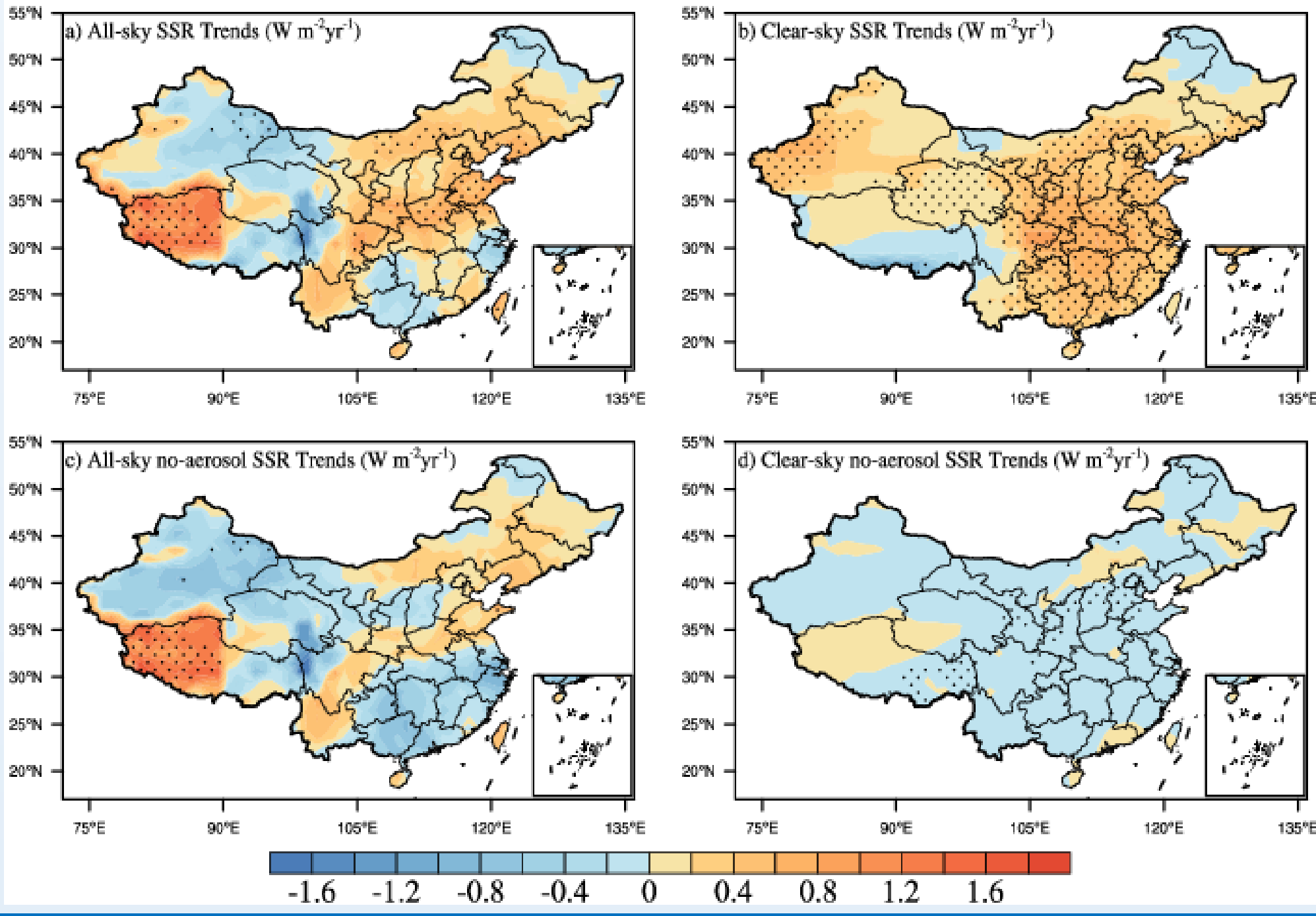


FIG. 1. Annual mean SSR trends under (a) all-sky, (b) clear-sky, (c) all-sky no-aerosol, and (d) clear-sky no-aerosol conditions from 2005 to 2018 over China based on CERES SYN products (unit: W m⁻² yr⁻¹). The dots represent significance at $\geq 95\%$ confidence level from the t-test.

Results - Comparisons of model-based and satellite-derived SSR trends

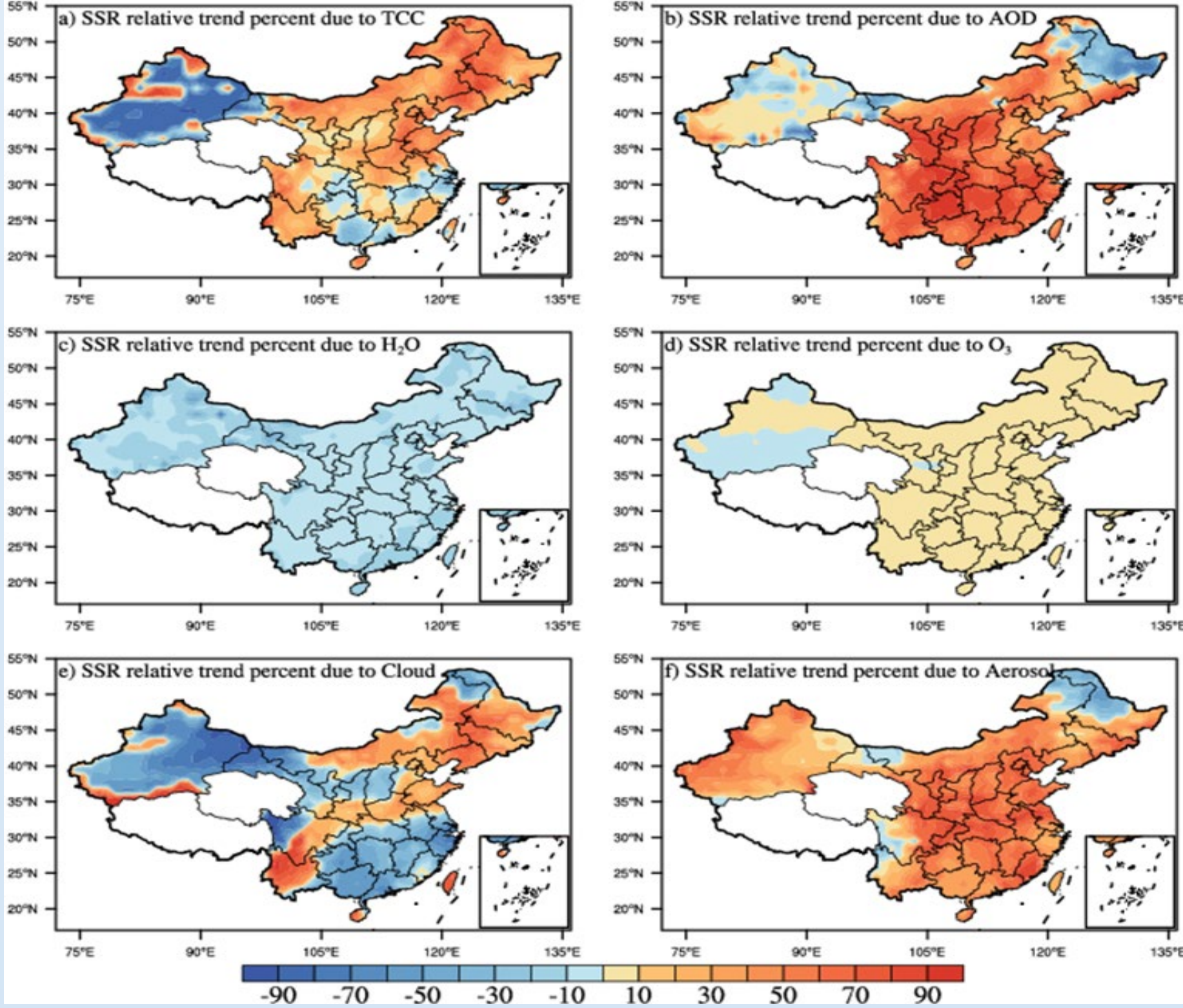


FIG. 3. Annual mean simulated SSR trend percentages (unit: %) due to (a) TCC, (b) AOD, (c) water vapor, and (d) ozone relative to all factors above from a single column radiative transfer model, as well as SSR trend percentages (unit: %) from (e) clouds and (f) aerosols derived from CERES SYN products (unit: unitless) during 2005-2018 over China.

Results - Annual and seasonal mean relative contributions from different cloud types to the cloud-cover-induced SSR trends

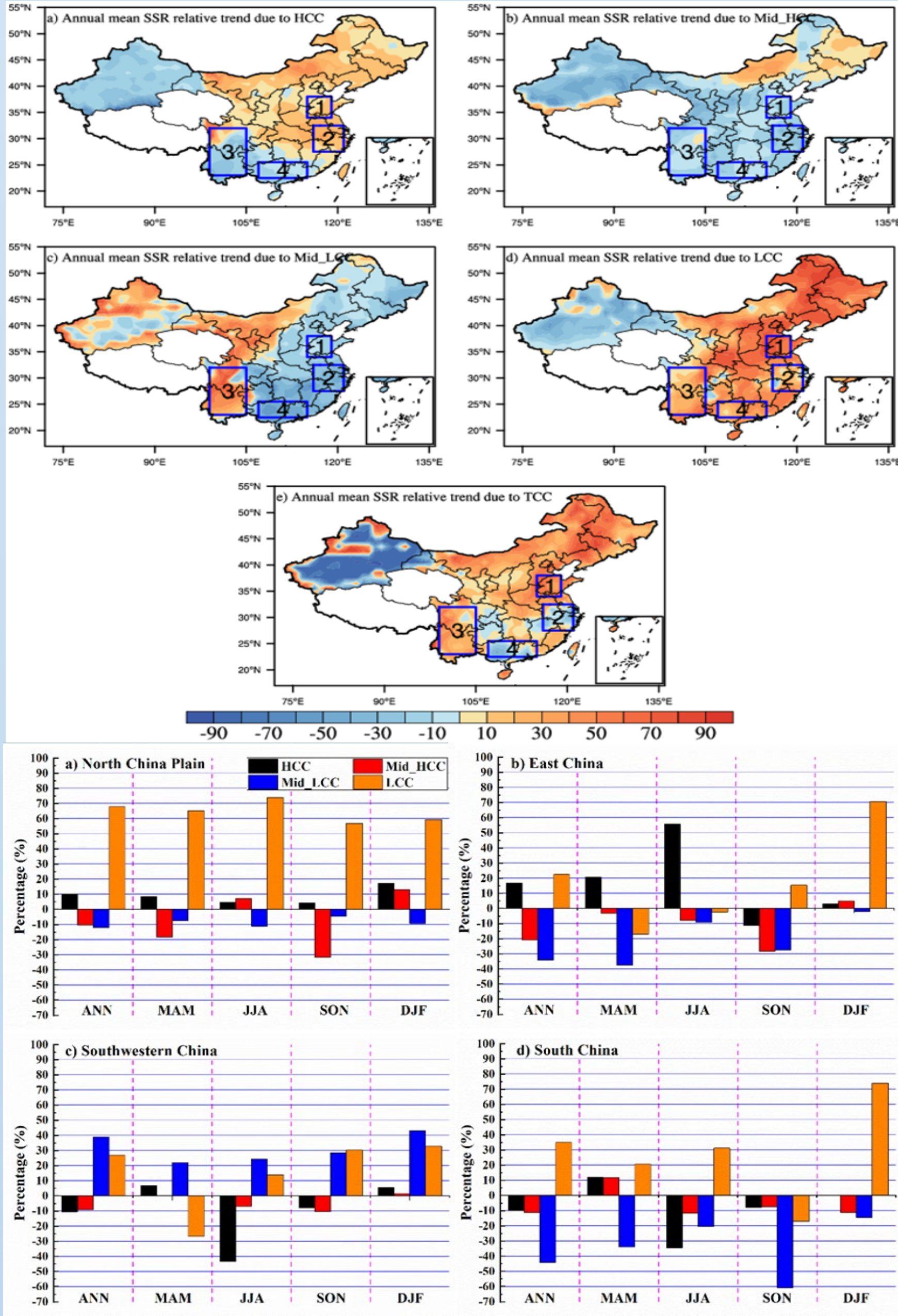


FIG. 4. Annual mean simulated SSR trend percentages (unit: %) due to (a) HCC, (b) mid-HCC, (c) mid-LCC, and (d) LCC relative to all cloud types, as well as simulated SSR trend percentage (unit: %) due to (e) TCC relative to all factors from 2005 to 2018 over China.

FIG. 5. Annual (ANN) and seasonal (MAM, JJA, SON, DJF) simulated SSR trend contributions (unit: %) from HCC (black), mid-HCC (red), mid-LCC (blue), and LCC (orange) relative to all cloud types averaged over four sub-regions for 2005-2018 in China, respectively, including (a) North China Plain, (b) East China, (c) Southwestern China, and (d) South China.